SEA ICE REMOTE SENSING WITH GNSS REFLECTIONS

F. Fabra[1], E. Cardellach[1], O. Nogués-Correig[1], S. Oliveras[1], S. Ribó[1], A. Rius[1], and M. Belmonte-Rivas[2]

[1]*Institut de Ciències de l'Espai (ICE-IEEC/CSIC), Campus UAB, Fac. Ciències Torre C5-par, 2on pis, 08193 Bellaterra, Spain*
[2]*KNMI, Royal Netherlands Meteorological Institute, Postbus 201, 3730 AE, De Bilt, Netherlands*

ABSTRACT

During the last polar winter, the GPS-SI experimental campaign was deployed in Greenland to collect GNSS reflected signals. The instrument employed has been the GPS Open Loop Differential Real-Time Receiver (GOLD-RTR), that gathers GPS signals in the form of 64-lags complex waveforms. During more than seven months, the complete process of sea-ice formation and melting has been continuously monitored, summing up to 1.4 TBs of data. This paper gives an overview of the most important aspects of this experiment and illustrates the remote sensing capabilities of the GPS-R concept to infer sea-ice properties, such as thickness, roughness and permittivity changes.

Key words: GNSS-R; Remote Sensing; Sea-Ice; Altimetry.

1. CAMPAIGN OVERVIEW

This work began in the frame of the GPS-SIDS project (funded by ESA and conducted by ICE-IEEC/CSIC, GFZ, IFAC/CNR, ADT), whose objective was to investigate the viability of using reflected GPS signals to study sea-ice and dry snow properties from space. For that purpose, it was required to obtain relatively long term high quality data sets using fixed platforms and then extrapolate the obtained results to a spaceborne platform. The logistics constraints in the Polar environments make this task more challenging than in other situations.

The GPS-SI experimental campaign started at the end of October 2008, taking place at Godhavn (Qeqertarsuaq), Disko Bay, Latitude 69°N, Greenland. The equipment was installed at a telecommunication tower situated at the edge of a cliff of approximately 650 meters high above sea level. The orientation of the site points the azimuthal field of view over the sea towards the South, where most of the GPS constellation lies at these latitudes. Due to the coastline profile, the range of elevations for GPS signals reflected off sea surface goes from 1° to 15° (Fig. 1). Under this conditions, our instrument has been able to monitor the formation, evolution and melting of sea-ice until mid of May 2009.

After introducing several aspects of the receiver and the experimental set-up, we present some of the techniques used to analyze the data, together with preliminary results.

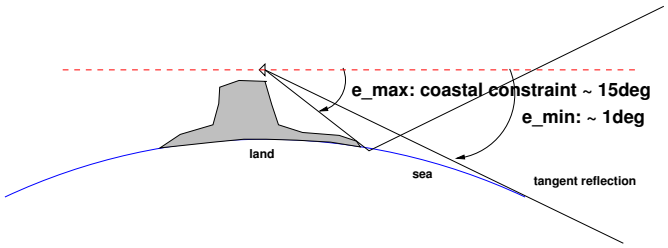

Figure 1. Visibility scenario. The minimum elevation is given by the ray that would reflect tangentially to the Earth surface, whereas the maximum elevation depends on the coastal separation.

2. THE RECEIVER: GOLD-RTR

The GOLD-RTR receiver [1] was designed, developed and tested at the CSIC/IEEC with the aim of collecting the GNSS signals reflected off the Earth's surface, from three different radio front-ends, and generate the complex cross-correlation function (waveform) in real-time. It has 640 complex correlators built in an FPGA and organized in 10 correlation channels. Each of them covers a delay-correlation window of 64 lags (corresponding to a 50 ns lag spacing), and can be tuned with ancillary Doppler and delay offsets. The equipment thus permits to produce up to 10 simultaneous delay-maps (DM), 1 delay-Doppler Map (DDM) with 10 frequency slices, or any combination of DM/DDM that requires 10 channels. The 3 front-ends are fed by one up-looking antenna for reference signal (direct), and either one or two other antennas (down-looking for reflected signals, either polarization). The GOLD-RTR has been widely used since 2005 [2, 3], and nowadays it has been replicated (3 additional GOLD-RTRs available).

The observables gathered by the GOLD-RTR can be classified as:

- Raw observables: 64-lag complex waveforms (I & Q), 15 meter inter-lag delay, at 1 millisecond coherent integration; their peak amplitude and phase. This level of data is required to built phase-related observables such as the phase-delay.
- Integrated observables: 64-lag amplitude waveforms, and their peak amplitude or power. The non-coherent integrated waveforms enhance the signal-to-noise level, although the phase information content is lost in the pro-

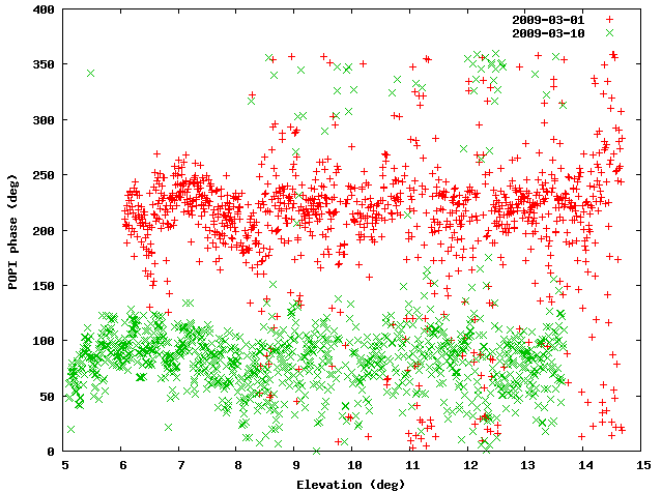

Figure 2. POlarimetric Phase Interferometry (POPI) of GNSS reflections over sea-ice for the same ground track (PRN 02), ten days apart. Besides a constant bias (instrumental), some features repeat. Variations in the presence of salinity may produce variations in the POPI.

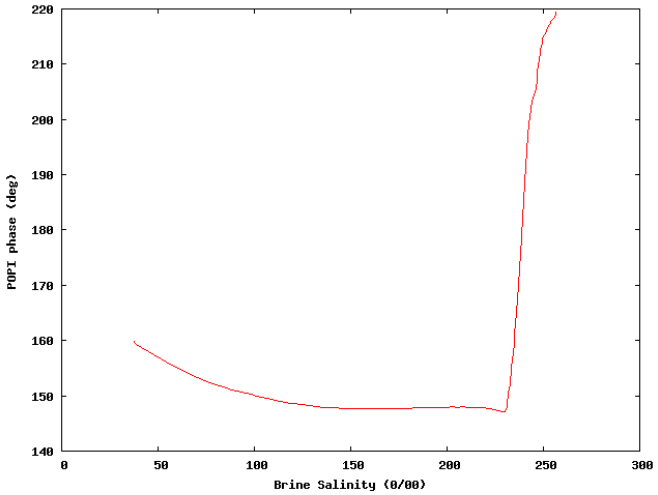

Figure 3. Phase difference between the co- and cross-polar Fresnel coefficients for sea-ice under presence of salinity, as modeled in [9].

cess. The shape of the waveform captures the diffuse scattering and links with the roughness and/or multi-path.

- Polarimetric observables: any combination of the complex and/or integrated observables taken with both co- and cross-polar components. An example is the Polarimetric Phase Interferometry (POPI, Fig. 2), differential phase between the co- and the cross-polar components of the reflected signals.

3. EXPERIMENTAL SET-UP

Two antennas were mounted on a tower for our purposes. The direct antenna (RHCP) was looking to the Zenith and was used to acquire direct GPS signals. By feeding the output of this antenna into link 1 of GOLD-RTR, the receiver was able to generate the open loop models used to perform the complex cross-correlation functions. A second dual-polarization antenna (RHCP-LHCP) was mounted looking horizontally, pointing to the open sea area to gather GPS signals reflected off the water surface. This reflection antenna had two ports, one for each polarization which were directly fed to links 2 and 3 of the GOLD-RTR.

The data collected was stored by a terminal unit (an industrial computer) linked with the receiver by an ethernet connection. Despite the high capacity of the hard drives and the use of compression algorithms, the record of raw observables had to be limited to two hours per day. Integrated waveforms were collected continuously and the total amount of data reached 1.4 TB. The terminal unit was also in charge of updating the configuration of the GOLD-RTR. The availability of internet connection during most of the campaign allowed us to operate remotely the equipment. A web interface was implemented for monitoring the collected data and the status of the instrument in real time. In addition, integrated observables were downloaded several times per day from the experimental site to our institute. The limitations in bandwidth made unfeasible to do the same with raw data.

4. REMOTE SENSING OF THE SEA-ICE

The sea-ice is typically characterized by its concentration, thickness, roughness, and presence of salinity. Different classifications exist, such as the percentage coverage (part of the surface covered by sea-ice); the form of the ice (size of the floes: pancake, growler, floe...); and the stage of development (thickness and age of the ice). The GNSS technique can potentially measure the sea-ice altimetry, which relates to the free-board parameter (altitude between the floating line and the free top surface), which in turn is linked to the total thickness. GNSS-R can also infer roughness properties, which should help characterizing the ice type, together with the presence of salinity. GNSS-R estimates of sea-ice types have been tackled in [4, 5], by means of the total reflected power (linked to permittivity) and waveform shape (roughness). Those works were conducted from aircrafts, and unlike our campaign, they used small incidence angles of observation. In the following paragraphs we discuss some other techniques applied to sea-ice reflected data for altimetric and salinity retrieval capabilities.

Observations done by UKDMC satellite [6] indicated the potential use of the phase coherence of the reflected GPS signals from sea-ice. As time goes by and the GNSS satellite moves across the sky, the incidence angle of the observation changes, and with it, the delay between the direct and reflected signal. This delay ρ depends on the altitude of the receiver above the reflecting surface H, as $\rho = 2H\sin(e)$ being e the elevation angle (complementary to the incidence, $90^\circ - \theta_{inc}$). Therefore, the evolution of the differential phase between direct and reflected signal could estimate the height of the receiver with respect to the specular surface. However, signal fading and multipath make this process difficult. To solve it, the approach followed has been to stop the phase by counterrotating the IQ vector with a combination of both geometric and atmospheric

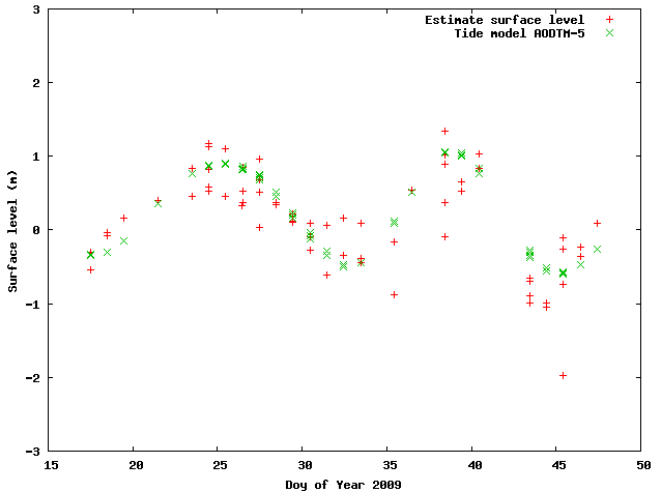

Figure 4. Comparison between surface level estimation given by the differential phase from PRN 07 (red) with the Artic Tide Model AODTM-5 (green).

delays. The IQ vector is obtained by multiplying the complex components from the peak of the reflected waveform with the conjugated equivalents from the direct signal. The geometric delay is computed by the relative distance between the path that goes from the satellite to the specular point and continues to the receiver, with respect to the satellite-to-receiver direct path. The position of both ends is known and the specular is computed over the geoid EGM96. The atmospheric delay is given by a global mapping function [7] and the Total Zenith Delay provided by GFZ. Once the differential phase is stopped, a linear fit is applied to estimate a residual height (ΔH), which can be interpreted as an estimation of the surface level. Fig. 4 shows an example of this estimation (red) and compares it with the Artic Tide Model AODTM-5 [8] (green) computed at the same time of the day. It can be seen a correlation between both results.

Since the differential stopped phase gives information about the surface level, its variation should be related with the roughness of that surface. Fig. 5 shows the root mean square of the stopped phase as a function of $\sin(e)$ (image on top) for a determined satellite and several days. The image at the bottom of the figure shows the ice concentration provided by daily ice charts from DMI, and interpolated to the locations of the specular points. A matching between the shape of both plots is noticeable.

The presence of salinity in the sea ice modifies its dielectric properties, resulting in different phase for the co- and cross-polar components of the complex Fresnel coefficients (Fig. 3). This difference is captured as the POlarimetric Phase Interferometry (POPI) [10], the phase-difference between the received co- and cross-polarized fields, or equivalently, the phase of their complex conjugate $E_r^{RHCP} E_r^{LHCP*}$. The GOLD-RTR system is not able to provide the absolute phases, because of the arbitrary a-priori phase used to set up each correlation channel at the beginning of a track-record. Nevertheless, variations in the POPI might relate to variations in the ice salinity. Two examples of POPI phase are shown in Fig. 2.

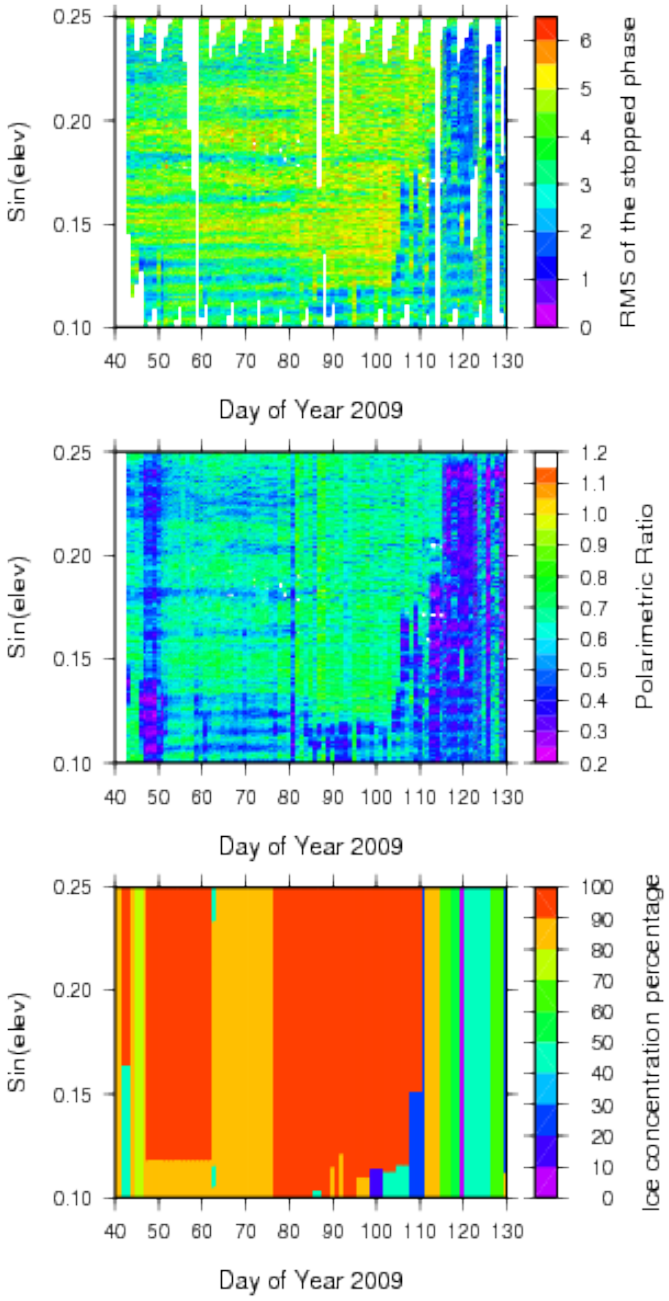

Figure 5. Different plots as a function of $\sin(e)$ *for several days: (Top) RMS of the stopped differential phase from PRN 02; (Middle) Polarization Ratio (RHCP/LHCP) from PRN 02; (Bottom) Ice concentration provided by DMI.*

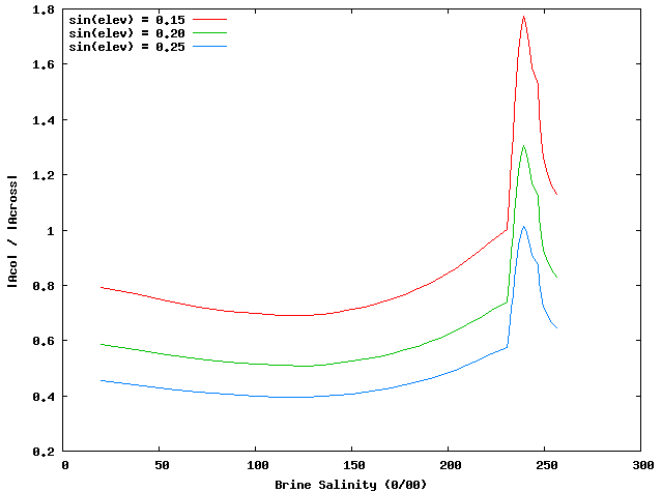

Figure 6. Amplitude ratio between the co- and cross-polar Fresnel coefficients for sea-ice under presence of salinity, as modeled in [9]. The result is elevation dependent.

Similarly, the Polarization Ratio between the co- and cross-polar components (RHCP/LHCP) should also relate to ice salinity variations (Fig. 6) . Fig. 5 shows this ratio computed with real data, as a function of $\sin(e)$ (image in the middle) for a determined satellite and several days. Again, there is also a matching with the shape of the ice concentration. Moreover, different satellite result in consistent behavior, as it can be seen in Fig. 7.

5. SUMMARY

This paper has shown several aspects about the GPS-SI campaign in Greenland, where the GOLD-RTR receiver has been used. Strategies for the characterization of sea-ice by means of the GNSS-R concept have been presented, giving emphasis to the study of the coherent phase for altimetric and roughness estimations and polarimetric measurements for the determination of the ice salinity variation. The work is still under progress and some preliminary results have been shown.

ACKNOWLEDGMENTS

This work has been done under contract ESA 21793/08/NL/ST, and Spanish Ministry of Science and Innovation ESP2007-30996-E and AYA2008-05906-C02-02. The campaign has been the effort of many individuals and organizations: ESA/ESTEC, ICE-IEEC/CSIC, GFZ, ADT, DMI, and discussions with Salvatore D'Addio (ESA/ESTEC).

REFERENCES

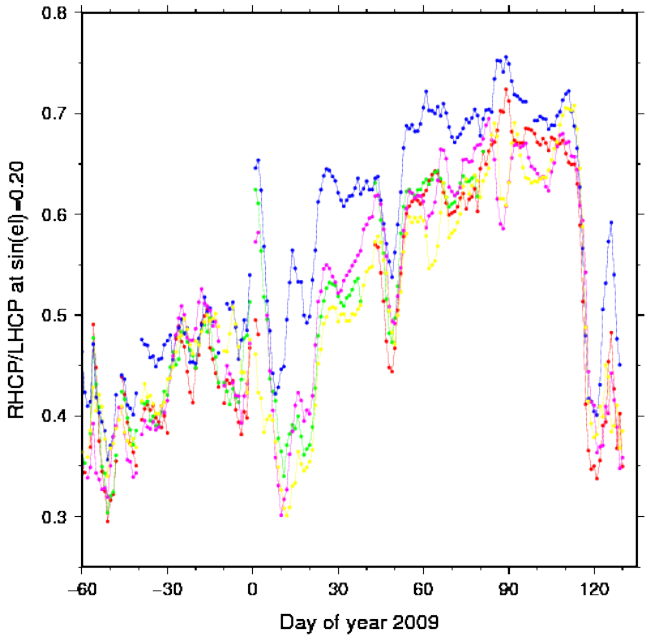

Figure 7. Polarization Ratio (RHCP/LHCP) for a given elevation angle and for different satellites (PRNs): 2-red, 5-green, 14-blue, 17-pink and 20-yellow.

[1] Nogués-Correig, O., E. Cardellach, J. Sanz, and A. Rius, "A GPS-Reflections Receiver that Computes Doppler/Delay maps in Real Time", IEEE Trans. Geosci. and Remote Sens., 45 (1), January 2007.

[2] Cardellach, E., A. Rius, "A new technique to sense non-Gaussian features of the sea surface from L-band bi-static GNSS reflections", Remote Sensing of Environment, Vol. 112, pp. 2927-2937, 2008.

[3] Rius, A., E. Cardellach, and M. Martín-Neira, "Altimetric Analysis of the Sea Surface GPS Reflected Signals", submitted to IEEE Trans. Geosci. and Remote Sens., 2009.

[4] María Belmonte Rivas, "Bi-Static Scattering of Global Positioning System Signals from Arctic Sea Ice", Ph.D. dissertation, University of Colorado, 2007.

[5] María Belmonte Rivas, J. A. Maslanik, P. Axelrad, "Bistatic scattering of GPS signals off Arctic sea ice", IEEE Trans. Geosci. and Remote Sens., Vol.48, Issue.1, doi:11.1109/TGRS.2009.2029342, 2009.

[6] S. Gleason, S. Hodgart, Y. Sun, C. Gommenginger, S. Mackin, M. Adjrad, and M. Unwin, "Detection and processing of bistatically reflected GPS signals from low earth orbit for the purpose of ocean remote sensing", IEEE Trans. Geosci. and Remote Sens., 43 (6), 2005.

[7] Boehm, J., A.E. Niell, P. Tregoning, H. Schuh, "Global Mapping Functions (GMF): A new empirical mapping function based on numerical weather model data", Geoph. Res. Letters, Vol. 33, L07304, doi:10.1029/2005GL025545, 2006.

[8] Padman, L., and S. Erofeeva, "A barotropic inverse tidal model for the Arctic Ocean", Geophys. Res. Lett., 31(2), L02303, doi:10.1029/2003GL019003, 2004

[9] Ulaby, F.T, R.K. Moore, and A.K. Fung, Microwave Remote Sensing Active and Passive, Artech House, Inc, 1986.

[10] Cardellach, E.,S. Ribó, and A. Rius. (2006,July). "Technical Note on POlarimetric Phase Interferometry (POPI)". ArXiv:physics [Online]. Available: http://arxiv.org/pdf/physics/0606099